Annals of Anatomy 250 (2023) 152141

Contents lists available at ScienceDirect

Annals of Anatomy

journal homepage: www.elsevier.com/locate/aanat

Research article

Postnatal morpho-functional development of a dog's meniscus

Silvia Clotilde Modina [a], Lucia Aidos [a], Valentina Rafaela Herrera Millar [b], Margherita Pallaoro [a], Umberto Polito [a], Maria Cristina Veronesi [a], Giuseppe Maria Peretti [b,c], Laura Mangiavini [b,c], Liliana Carnevale [a], Federica Boschetti [c,d], Francesco Abbate [e], Alessia Di Giancamillo [b,*]

[a] Department of Veterinary Medicine and Animal Science, University of Milan, Via dell'Università, 6, 26900 Lodi, Italy
[b] Department of Biomedical Sciences for Health, University of Milan, Via Mangiagalli, 31, 20133 Milan, Italy
[c] IRCCS, Ospedale Galeazzi – Sant'Ambrogio, Via Cristina Belgioioso 173, 20157, Milan, Italy
[d] Department of Chemistry, Materials and Chemical Engineering "Giulio Natta", Polytechnic University of Milan, 20133 Milan, Italy
[e] Department of Veterinary Sciences, University of Messina, Polo Universitario S.S. Annunziata, 98168 Messina, Italy

ARTICLE INFO

Article history:
Received 20 March 2023
Received in revised form 4 July 2023
Accepted 10 July 2023
Available online 25 July 2023

Keywords:
Meniscus morphology
Development
GAGs
Collagen fibers
Dog

ABSTRACT

This study evaluates the morpho-functional modifications that characterize meniscal development from neonatal to adult dogs. Even if menisci are recognized as essential structures for the knee joint, poor information is available about their morphogenesis, in particular in dog models. Menisci from a group of Dobermann Pinchers aged 0, 10, 30 days, and 4 years (T0, T10, T30, adult, respectively) were analyzed by SEM, histochemistry (Safranin O and Picro Sirius Red Staining analyzed under a polarized light microscope), immunofluorescences (collagen type I and II), biomechanical (compression) and biochemical analyses (glycosaminoglycans, GAGs, and DNA content). SEM analyses revealed that the T0 meniscus is a bulgy structure that during growth tends to flatten, firstly in the inner zone (T10) and then even in the outer zone (T30), until the achievement of the completely smooth adult final shape. These results were further supported by the histochemistry analyses in which the deposition of GAGs started from T30, and the presence of type I birefringent collagen fibers was observed from T0 to T30, while poorly refringent type III collagen fibers were observed in the adult dogs. Double immunofluorescence analyses also evidenced that the neonatal meniscus contains mainly type I collagen fibers, as well as the T10 meniscus, and demonstrated a more evident regionalization and crimping in the T30 and adult meniscus. Young's elastic modulus of the meniscus in T0 and T10 animals was lower than the T30 animals, and this last group was also lower than adult ones (T0-T10 vs T30 vs adult). Biochemical analysis confirmed that cellularity decreases over time from neonatal to adult ($p < 0.01$). The same decreasing trend was observed in GAGs deposition. These results may suggest that the postnatal development of canine meniscus may be related to the progressive functional locomotory development: after birth, the meniscus acquires its functionality over time, through movement, load, and growth itself.

1. Introduction

To date, meniscal pathology treatment focuses on eliminating the damaged portion of the meniscus, but also on rebuilding it or even replacing it. This goal is, however, still far from its prompt fulfillment, even if many attempts have already been made (Ding and Huang, 2015; Yu et al., 2015). For this reason, further studies are needed to deepen the knowledge of this small, but essential structure. The composition, structure, and biomechanics of the meniscus are fundamental building blocks for engineering meniscal tissue substitutes, since they all play a pivotal role in meniscal function and health, guaranteeing the correct activity of the knee joint.

Joint motion and the postnatal biomechanical stress of weight-bearing are the principal factors that determine architectural changes during the maturation of the meniscus, involving cell phenotype, the vascular network and the matrix composition (Deponti et al., 2015; Di Giancamillo et al., 2014; Di Giancamillo, Herrera Millar et al., 2017, 2021; Peretti et al., 2019). Different studies were

* Corresponding author.
E-mail address: alessia.digiancamillo@unimi.it (A. Di Giancamillo).

https://doi.org/10.1016/j.aanat.2023.152141

Table 1
Medial menisci from both right and left limbs were used; in each analysis, different animals were used so to avoid duplication of the experimental unit.

Time point	n° of collected dogs	SEM		Histochemistry, Immunofluorescence		Biomechanics		Biochemistry	
		Animal ID	Used Joint	Animal ID	Used Joint	Animal ID	Used Joint	Animal ID	Used Joint
T0	9	1	Right	1	Left	5	Left	4	Left
				2	Left	6	Left	6	Right
		2	Right	3	Right	7	Right	7	Left
				4	Right	8	Left	8	Right
		3	Left	5	Right	9	Left	9	Right
T10	6	1	Right	1	Left	3	Left	3	Right
						4	Left	4	Right
		2	Left	2	Right	5	Right	5	Left
						6	Right	6	Left
T30	6	1	Right	1	Left	3	Left	3	Right
						4	Left	4	Right
		2	Left	2	Right	5	Right	5	Left
						6	Right	6	Left
Adult	6	1	Right	1	Left	3	Left	3	Right
						4	Left	4	Right
		2	Left	2	Right	5	Right	5	Left
						6	Right	6	Left

performed in animal models (murine and chicken) and human embryos. These studies reported that meniscus formation happens at 8 days in chicken embryos (Mikic et al., 2000), at 15 days in mice embryos (Gamer et al., 2017), and as early as 7 weeks of gestation in human embryos (Uhthoff and Kumagai, 1992).

Mice models provided useful information about the embryologic development of the meniscus. In this species, menisci originate from a condensation of cells present in the interzone, the area of the future formation of the knee joint (Gamer et al., 2017; Hyde et al., 2008). Medial and lateral menisci derive from two different cell strains of the joint embryonic gem: the cells that compose the inner zone of the medial meniscus derive from resident cells of the anlagen, that momentarily switch off the expression of collagen type II (typical of the cartilaginous tissue) to form the interzone at day 13.5 of embryo's development; on the other hand, the lateral meniscus and the outer medial meniscus derive from cells that invade the developing knee joint, from the area adjacent to the interzone at day 14.5. In mice, at birth, the double nature of the meniscus is already evident with an outer vascular zone, composed of elongated fibroblast-like cells and an avascular inner zone with round fibro-chondrocytes within an Extracellular Matrix (ECM) rich in proteoglycans (PGs). Moreover, in the superficial zone of the meniscus, adjacent to the articular cartilages of the femur and tibia, ovoid-shaped cells are present in about 1–2 cells thick layers (Gamer et al., 2017; Sosio et al., 2015). This zone becomes smooth and intact at 1 week of age, which concurs with the starting point of the expression of type II collagen by the inner region and the superficial zone cells (Gamer et al., 2017). Similar patterns of postnatal meniscal maturation have been described in swine (Di Giancamillo et al., 2014) and ovine (Melrose et al., 2005) models, and also in the human meniscus, as reviewed (Fox et al., 2012; Makris et al., 2011). Few studies are focused on meniscal pre- and post-natal morphogenesis, both in human (Fukazawa et al., 2009; Koyuncu et al., 2017) and animal models (Di Giancamillo et al., 2014; Gamer et al., 2017; Hyde et al., 2008; Makris et al., 2011; Tsinman et al., 2021). Whatever model is chosen, it is necessary to keep in mind that differences exist between humans and animals, e.g. different types of locomotion (bipedal vs quadrupedal) or the diverse time points of tissue maturation: a perfect animal model for humans is still lacking (Proffen et al., 2012; Ribitsch et al., 2018).

Dogs constitute a valid species for translational studies, as their microscopic and macroscopic meniscal anatomy is similar to that of humans and as they develop spontaneous knee pathologies (Krupkova et al., 2018). It also must be considered that the dog is often subject to pathologies of the medial meniscus as a consequence of the rupture of the anterior cranial ligament of the knee: the resulting joint instability causes damage to the medial meniscus in 53–74% of cases (Frost-Christensen et al., 2008). Anatomically, the medial meniscus is more firmly attached to the tibial plateau than the lateral one and for this reason, an abnormal joint motion will cause shear forces on it (Frost-Christensen et al., 2008).

Moreover, dogs could work as a potential model to better understand meniscal biology and development. It would be interesting 1) to investigate how connective tissues respond to mechanical stress; 2) study the developmental biology of the meniscus as a function of future reparative or regenerative applications; and 3) obtain a model useful for translational medicine. Mechanical load plays a central role in the proper functioning of the meniscus, and may as well have an influence on the balance of ECM in both humans and dogs (McNulty and Guilak, 2015). Many studies demonstrated that the biomechanical properties of the meniscus vary according to the site (anterior, middle, and posterior) and depth (Danso et al., 2017; Peretti et al., 2019; Proctor et al., 1989). Moreover, the fiber structure which is made of two orthogonal collagenous networks, radial and circumferential, may also contribute to the same mechanical properties.

Therefore, the aim of the present study was to characterize the morphological, structural, biochemical, and biomechanical properties of the canine medial meniscus during growth, from birth to adulthood.

The medial meniscus was chosen since it is the more frequently injured.

2. Material and methods

2.1. Study design

The postnatal morphogenesis of canine medial menisci was evaluated, focusing on collagen fibers arrangement and matrix deposition, in a population of neonatal to adult dog cadavers. For each analysis, medial meniscus samples from the right and left limbs of each animal were used, assuring to use different animals, to avoid the duplication of the experimental unit (Table 1); moreover, the research regards only medial menisci since they are more frequently injured than lateral ones (Case et al., 2008).

At birth (T0; n = 9 dogs, 18 medial menisci), 10 days (T10, n = 6 dogs, 12 medial menisci), 30 days (T30, n = 6 dogs, 12 medial menisci), and 4 years old (adult, n = 6 dogs, 12 medial menisci) dog's cadavers were evaluated. To avoid inter-breed variances, only animals belonging to the same (large) breed were used: Dobermann Pinscher (adult

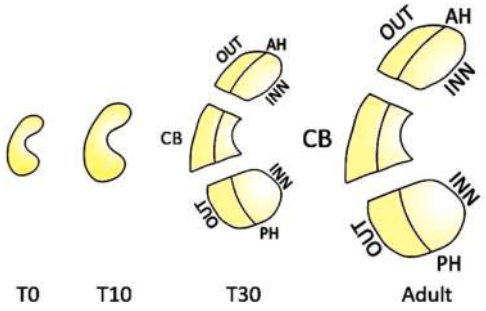

Fig. 1. Schematic representation of the menisci subdivision. Two radial cuts were performed in three sections: the anterior (AH) and posterior (PH) horns and the central body (CB). Moreover, the inner (INN) or outer (OUT) parts are labelled.

weight > 35 kg). No animal was sacrificed for research purposes, moreover, the chosen dogs showed no signs of orthopedical diseases that could interfere with the performed analyses. Considering the absence of pathologies, the left or right joint were distributed to each assay randomly: in fact, no difference is expected between the left and right joint. The cadavers used in the present study followed the guidelines of the E.U directive 2010/63/EU. After the owner informed consent, each sample was harvested, and capsular tissue and ligaments were removed. Afterwards, menisci of 30-day old dogs and adult dogs were subdivided with two radial cuts into their three typical anatomical portions: the anterior and posterior horns (AH and PH, respectively) and the central body (CB) (Fig. 1).

2.2. Scanning Electron Microscopy (SEM)

Medial menisci for each age (n = 3 in T0, n = 2 in T10, T30, and adult, total specimens =9 menisci) were evaluated as a whole through Electronic Scan Microscopy (SEM, Zeiss EVO LS 10, Carl Zeiss NTS, Germany). Samples were fixed in 2.5% glutaraldehyde in Sorensen phosphate buffer 0.1 M, after several rinsing in the same buffer, they were dehydrated and critical-point dried in a Balzers CPD 030, sputter coated with 3 nm gold in a Balzers BAL-TEC SCD 050 and examined under a Zeiss EVO LS 10 scanning electron microscope.

2.3. Morphological analyses: histochemistry and double immunofluorescence

Medial menisci from T0, T10, T30, and adult dogs (n = 5 in T0, n = 2 in T10, T30, and adults, total specimens=11 menisci) were sampled and fixed in buffered 10% formalin (Bio-Optica, Milan, Italy) for 24 h, dehydrated and embedded in paraffin. Microtome longitudinal Section (4 μm thickness) of the entire tissue (T0 and T10 samples) or portioned meniscus (AH, CB or PH, T30 and adult samples) were analyzed for describing both meniscal structure and GAGs deposition in the matrix. For each sample, some sections were analyzed using polarized light microscopy (Optika B-510BF, Olympus, Opera Zerbo, Milan, Italy) after Picro Sirius Red Staining to assess the spatial orientation of the collagen networks, highlighted by the birefringence of the fibers to observe collagen type I and III. Other sections were stained with Safranin O to highlight the GAGs presence within the tissue. Sections were analyzed with an Olympus BX51 light microscope (Olympus, Opera Zerbo, Milan, Italy) equipped with a digital camera.

Double immunofluorescence was performed to reveal the localization and the possible co-localization of collagens type I and II. After rehydration, heat-induced antigen retrieval was performed (citrate buffer pH 6, five minutes microwaves 500 W, followed by cooling, twice). After washing three times in Phosphate buffer saline (PBS, pH 7.4), treatment with the Avidin–Biotin blocking kit solution (Vector Laboratories Inc., Burlingame, CA USA) was performed. Sections were incubated with the first-step primary antiserum, 1:50 collagen type I (Cat n. AB233080, rabbit polyclonal, Abcam, Cambridge, UK) for 24 h at 18–20 °C and washed in PBS. The sections were incubated with a solution of goat biotinylated anti-rabbit IgG (Vector Laboratories Inc.), 10 μg/ml in PBS for 1 h at 18–20 °C. After rinsing twice in PBS, the sections were treated with Fluorescein–Avidin D (Vector Laboratories Inc., Newark, USA), 10 μg/ml in NaHCO3, 0.1 M, pH 8.5, 0.15 M NaCl for 1 h at 18–20 °C. For the second step of the double immunofluorescence procedure, sections were treated in a 2% hyaluronidase solution at room temperature for 30 min. Slides were subsequently treated with 1:50 anti-collagen type II antiserum (Cat. n. 20333, Chondrex Inc., Redmond, WA, USA) overnight. Sections were rinsed in PBS for 10 min and incubated with 10 μg/ml goat biotinylated anti-mouse IgG (Vector Laboratories Inc., Newark, USA) for 1 h at 18–20 °C. The sections were then washed twice in PBS, and treated with Rhodamine–Avidin D (Vector Laboratories Inc. Newark, USA), 10 μg/ml in NaHCO3, 0.1 M, pH 8.5, with 0.15 M NaCl for 1 h at 18–20 °C. Finally, slides with tissue sections were embedded in Vectashield Mounting Medium with DAPI (SKU H-1200–10, Vector Laboratories Inc., Newark, USA) and observed using a Confocal Laser Scanning Microscope (FluoView FV300; Olympus). The immuno-fluo-reactive structures were excited using Argon/ Helio–Neon–Green lasers with excitation and barrier filters set for fluorescein and rhodamine. Images containing superimposition of fluorescence were obtained by sequentially acquiring the image slice of each laser excitation or channel. In the double immunofluorescence experiment, the absence of cross-reactivity with the secondary antibody was verified by omitting the primary antibody during the first incubation step.

2.4. Biomechanical analysis

Differences between ages during animal growth in response to compression with Unconfined Young's Ec were tested (n = 5 in T0, n = 4 in T10, T30, and adults, total specimens=17 menisci). The elastic unconfined compressive modulus (Ec) was evaluated using EnduraTEC ELF® 3200 machine (TA Instrument, New Castle, DE, USA), equipped with a 22 N load cell. Menisci were used as follows: T0 as a whole because of their small dimension, while T10, T30, and adult menisci were radially sectioned in the same three portions (AH, CB, and PH), stored in saline solution NaCl 0.9% and frozen at − 80 °C until time of testing. At least 24 h before test execution, samples were taken to a temperature of − 24 °C and then completely thawed at room temperature (23 °C). Subsequently, for each zone, a cylindrical part was cut as previously described by (Polito et al., 2020). The diameter of the samples was dependent on size of the original meniscus. Before testing, dimensional measurements on the samples were taken with a digital calliper to normalize data before statistical analysis. Briefly, the samples were introduced into a Plexiglas cell and PBS solution was added into the cell to avoid dehydration of the tissue. The thickness of all samples was measured from the position of the testing machine actuator, after imposing a preload of approximately 0.01 N. The sample was then subjected to a multi-ramp stress relaxation test, made of five increasing 4% strains at a velocity of 0.1%/s, followed by stress relaxation to equilibrium for 600 s. The compressive Ec was obtained for each ramp from the equilibrium data as the ratio between values of relaxation stress and the corresponding values of strain. The value of the Ec returned by each specimen during a compression rate of 12%, was considered representative.

2.5. Biochemical analysis

Biochemical analysis was performed on all groups (n = 5 in T0, n = 4 in T10, T30, and adults, total specimens=17 menisci). T0 menisci

were processed as a whole because of their small dimension, while T10, T30, and adult menisci were radially sectioned in AH, CB, and PH; they were digested in papain (Sigma-Aldrich, Milan, Italy) for 16–24 h at 60 °C: 125 mg/ml of papain in 100 mM sodium phosphate, 10 mM sodium EDTA (Sigma-Aldrich, Milan, Italy), 10 mM cysteine hydrochloride (Sigma-Aldrich, Milan, Italy), 5 mM EDTA adjusted to pH 6.5 and brought to 100 ml of solution with distilled water. Later, the digested samples were assayed separately for proteoglycan and DNA contents. Proteoglycan content was estimated by quantifying the amount of sulfated glycosaminoglycans using the 1,9-dimethylmethylene blue dye binding assay (Polysciences, Inc., Warrington, PA) and a microplate reader (wavelength: 540 nm). The standard curve for the analysis was generated by using bovine trachea chondroitin sulfate A (Sigma-Aldrich, Milan, Italy). DNA content was evaluated with the Quant-iT Picogreen dsDNA Assay Kit (Molecular Probes, Invitrogen, Carlsbad, CA, USA) and a fluorescence microplate reader and standard fluorescein wavelengths (excitation 485 nm, emission 538 nm, cut-off 530 nm). The standard curve for the analysis was generated using the bacteriophage lambda DNA supplied with the kit. To evaluate cell efficiency, the ratio between the amount of GAGs and DNA content was calculated.

2.6. Statistical analysis

Two different statistical analyzes were performed to better describe the results regarding biomechanics and biochemistry (Compressive forces and GAGs, DNA, GAGs/DNA ratio). First of all, the data obtained at each experimental time point (T0, T10, T30, and adult) were considered and a comparison was made between the means after the evaluation of their distribution (D′ Agostino & Pearson, Shapiro-Wilk and Kolmogorov-Smirnov normality test). When the data were normally distributed, a One-Way ANOVA was performed, otherwise, the Kruskal-Wallis test was applied. After that, a Two-Way ANOVA was performed to verify the effect of the meniscal portion under consideration (anterior horn, posterior horn, and central body) as the age varied. The data were analyzed with GraphPad Prism 6. The individual meniscal samples were the experimental unit of all response variables (Table 1). The data were presented as means ± S.E.M. Differences between means were considered significant at $p < 0.05$.

3. Results

3.1. Electronic Scan Microscopy

SEM imaging allowed us to see the different shapes of dog meniscus during growth. T0 meniscus is characterized by the presence of a bulgy structure (Fig. 2A, pink arrow) that during growth tends to flatten, firstly in the inner zone (T10 meniscus, Fig. 2B, white arrow) and then even in the outer zone (T30 meniscus, Fig. 2C, green arrow) until the achievement of the completely smooth adult final shape (Fig. 2D).

3.2. Morphological analyses: histochemistry

The morphological analyses were carried out on all portions of the medial meniscus (AH, CB, and PH). The results of the posterior horn were illustrated in Fig. 3 and Fig. 4, since it is the more easily injured portion (Case et al., 2008). Through the polarized light microscopy evaluation, it was possible to establish that the bulges are formed by collagen fibers that assume a yarn-like conformation (previously seen in Fig. 2A-B) that protrude from the surface of the

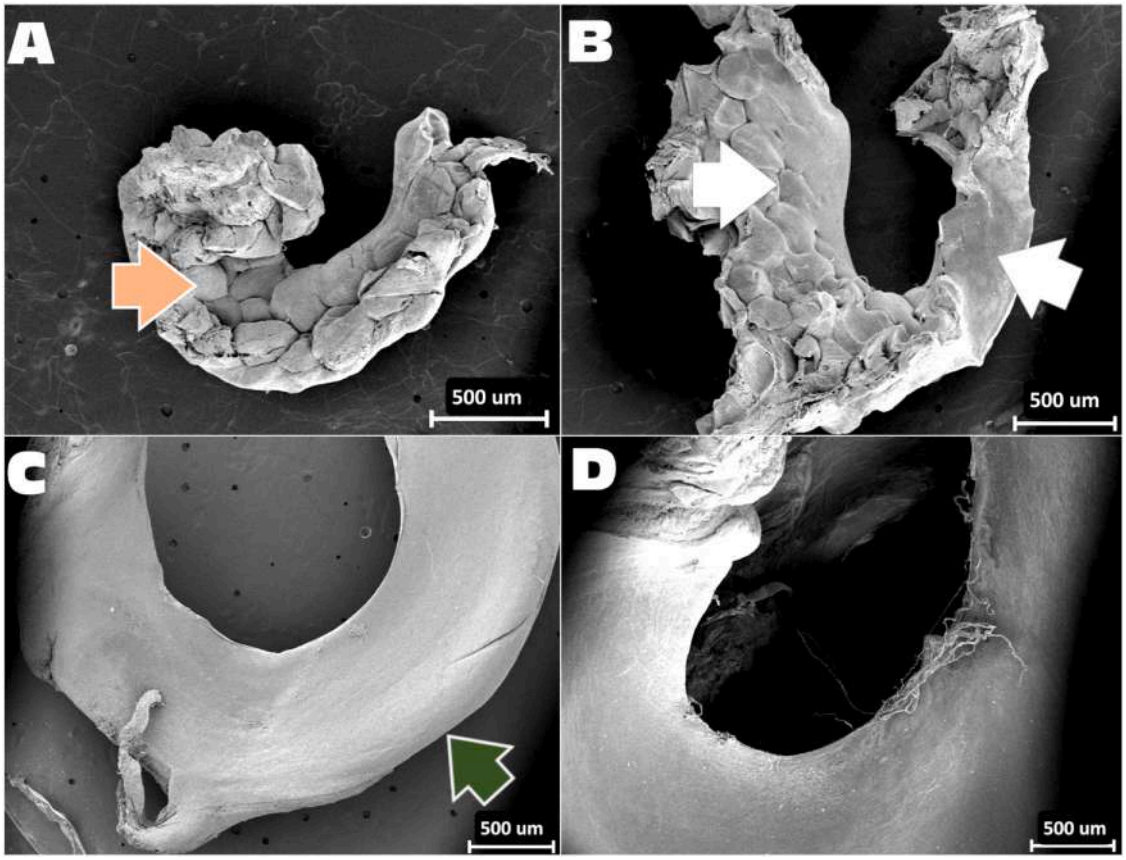

Fig. 2. Representative SEM images. A) T0 – medial meniscus. B) T10 – medial meniscus. C) T30 – medial meniscus. D) Adult – medial meniscus. Pink arrow = bulgy structure. White arrows = flattened zone. Green arrow = outer zone. Scale bar: 500 µm.

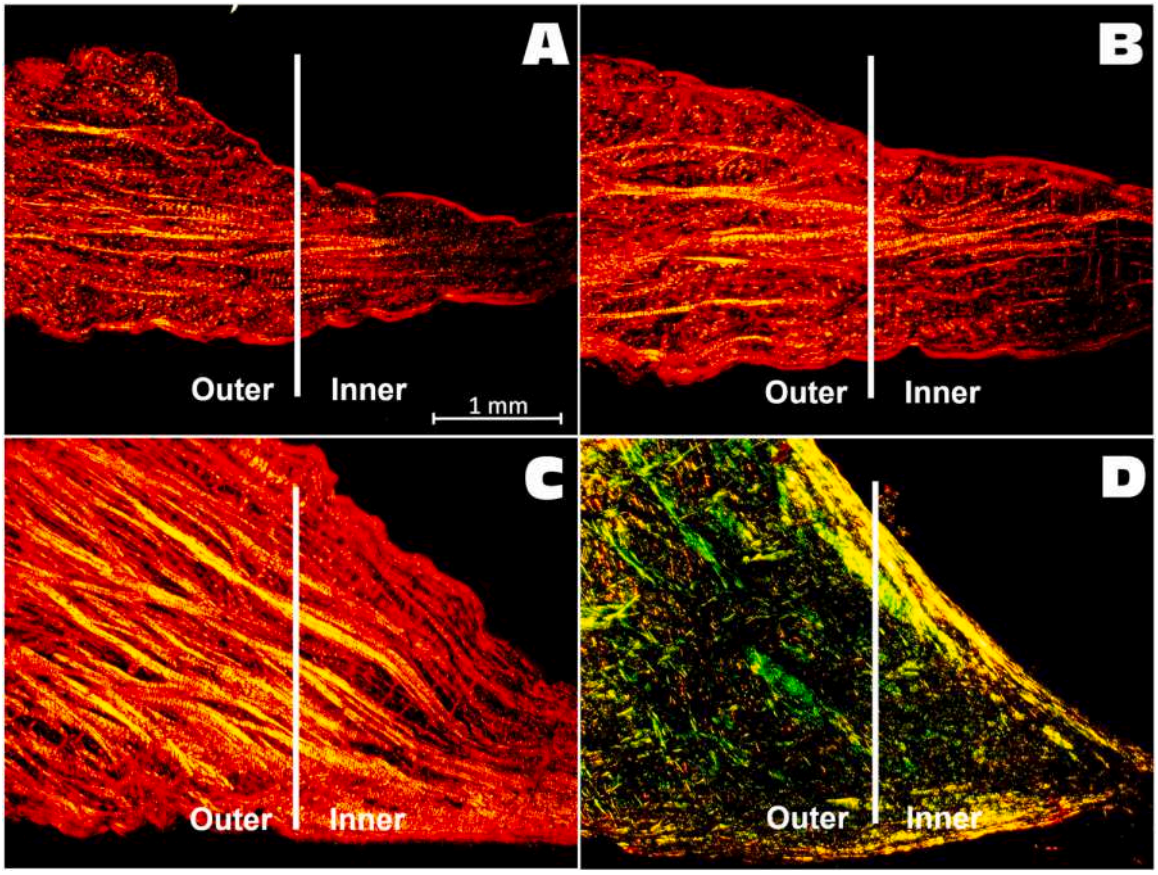

Fig. 3. Picro Sirius Red Staining of canine medial meniscus. A) T0 – medial meniscus, posterior horn. B) T10 – medial meniscus, posterior horn. C) T30 – medial meniscus, posterior horn. D) Adult – medial meniscus, posterior horn. Red-yellow fibers represented collagen type I and green fibers with weak birefringence represented collagen type III. Scale bar: 1 mm.

meniscus in the first phases of development (T0 and T10; Fig. 3A and Fig. 3B). Picro Sirius Red Staining revealed bright, red-yellow, and well-oriented collagen fibers, with a crimp pattern, parallel to the long axis of the meniscal wedge at T0, T10, and T30 (Figs. 3A, 3B, 3C, respectively). On the contrary, the adult meniscus revealed green collagen fibers (Fig. 3D).

Safranin O Staining (pink orange color, specific for proteoglycans, including GAGs) showed how cell morphology and matrix composition vary during growth. T0 meniscus was characterized by fibroblast-like cells in the outer zone (Fig. 4A1, black arrows) and a huge number of elongated cells (fibroblast-like cells, Fig. 4A2, white arrows) and no GAGs in the inner zone; T10 meniscus was very similar to the previous ones, with fibroblast-like cells still present in the outer zone (Fig. 4B1, black arrows); no GAGs were evident but some rounded cells began to be present in the inner zone (Fig. 4B2, asterisk). In the T30 meniscus fibroblast-like cells in the outer zone were still present (Fig. 4C1, black arrows), while in the inner zone, the rounded shape of the nuclei was more displayed (Fig. 4C2, asterisk), in association with the presence of slight matrix deposition (Fig. 4C2, hashtag). All these features were more evident in the adult meniscus where cells assumed a fibro (Fig. 4D1, black arrows) and/or chondrocyte-like (Fig. 4D2 asterisk) shape and cartilaginous-like matrix production was clearly visible both in the outer (Fig. 4D1, black arrows) and inner (Fig. 4D2 asterisk) zones.

3.3. Morphological analyses: double immunofluorescence

The menisci structure and organization, via double immunofluorescence (Fig. 5) has been studied and it was possible to recognize different aspects of menisci maturation.

Cellularity was higher at T0 and T10 (blue nuclei, Fig. 5A1 and Fig. 5B1, respectively, as confirmed by biochemical analyses (Fig. 7), while, starting from T30, the cellularity began to decrease (blue nuclei, Fig. 5C1 and 5D1) down to the lowest presence of cells in the adult (blue nuclei, Fig. 5E1, F1).

Collagen fiber staining revealed that the T0 meniscus contains mainly collagen type I fibers (green color, Fig. 5A2) as well as T10 menisci (green color, Fig. 5B2) and acquired a more evident regionalization and crimping in the T30 meniscus with collagen type I and II co-expression: it was possible to differentiate the inner zone, by the presence of collagen type I/II fibers co-localization (yellow, Fig. 5D2), from the outer zone, that presents a higher presence of collagen type I (yellow with a higher presence of green color, Fig. 5C2).

The same regionalization persisted, and it was magnified in adult meniscus: the double nature of the meniscus was highlighted by the presence of a cartilaginous-like inner zone, in which a clear chondrocyte-like phenotype may be recognized (red collagen type II, Fig. 5F2). Moreover, the outer fibrous zone was characterized by the expression of very crimped collagen type I additional to collagen II fibers (red collagen type II, and green collagen type I, Fig. 5E2).

3.4. Biomechanical analyses

Biomechanical analyses of the meniscus, as a whole, indicated that menisci from T0 and T10 were very similar. The compressive Young's elastic modulus of these two groups resulted to be lower than the one in T30; similarly, the modulus of this group was lower than the one scored for the adult (Fig. 6A, T0, T10 vs T30 vs adult, $p < 0.01$). The same trend was also observed when analyzing the different three meniscal areas: AH, CB, and PH (Fig. 6B; $p < 0.01$).

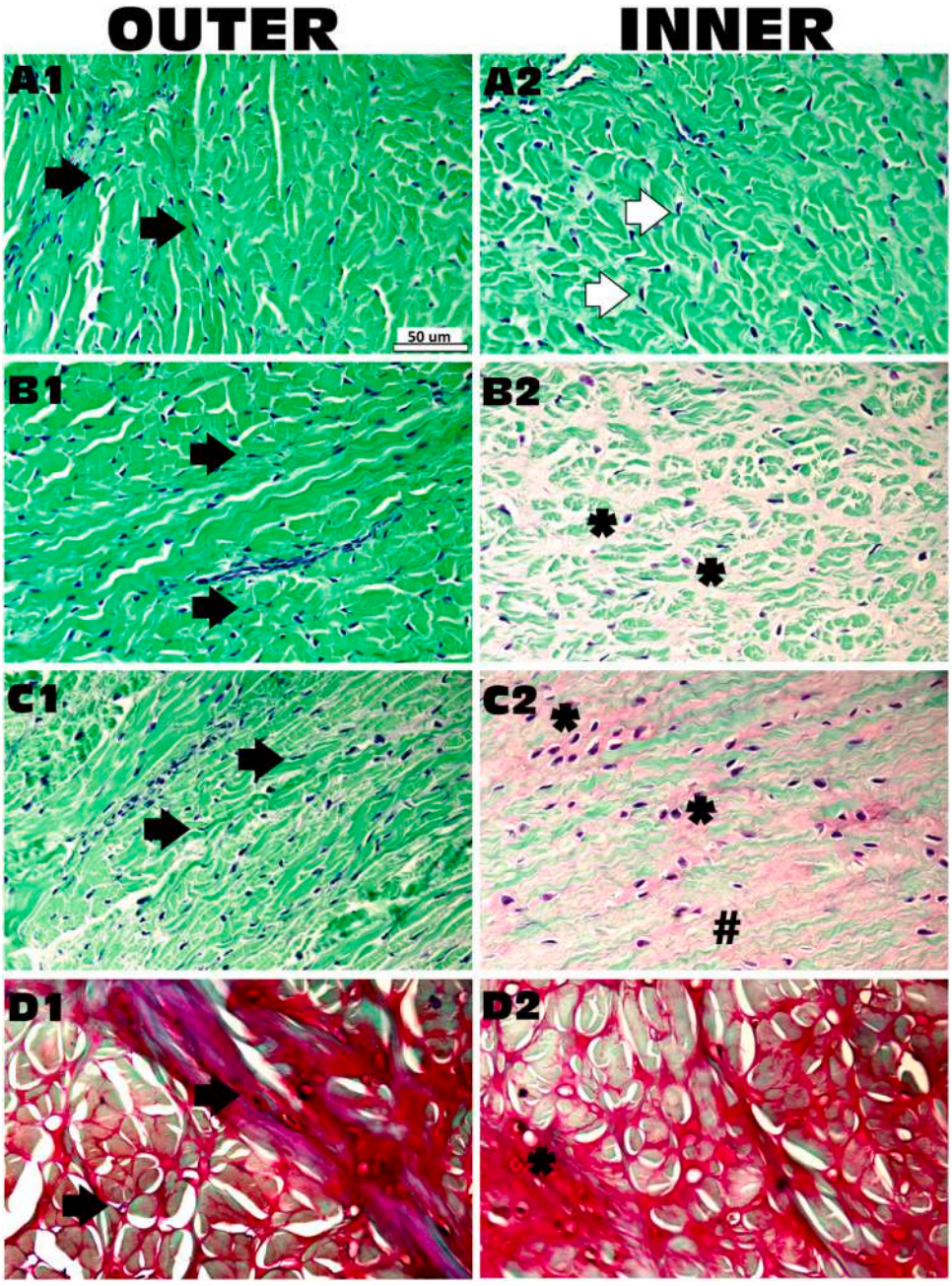

Fig. 4. Safranin O Staining of canine medial meniscus. A1) T0 – medial meniscus, posterior horn, outer zone. A2) T0 – medial meniscus, posterior horn, inner zone. B1) T10 – medial meniscus, posterior horn, outer zone. B2) T10 – medial meniscus, posterior horn, inner zone. C1) T30 – medial meniscus, posterior horn, outer zone. C2) T30 – medial meniscus, posterior horn, inner zone. D1) Adult – medial meniscus, posterior horn, outer zone, fibroblast-like cells. D2) Adult – medial meniscus, posterior horn, inner zone. Black arrows = chondrocyte-like cells. White arrows = elongated fibroblast-like. Asterisks = chondrocyte-like cells. Hashtag = cartilaginous-like matrix production, pale pink to pink orange color. Scale bar = 50 µm.

3.5. Biochemical analyses

Biochemical analysis was performed in all the samples as a whole, or the three portions AH, CB, and PH. The production of GAGs decreased significantly at all studied time points ($p < 0.001$ in T10 vs T0, $p < 0.001$ in T30 vs T10, $p < 0.05$ in adult vs T30, Fig. 7A). The same trend of GAGs was seen regarding the meniscal areas (Fig. 7B): in all three meniscal areas, there were statistical differences between all age groups ($p < 0.05$, Fig. 7B), except for the T30 and adult groups, where no statistical differences were found, indicating that these age groups show the same GAGs production.

The same decreasing trend was observed in cellularity over time (Fig. 7C): the T0 DNA content could be compared with the T10 menisci, with no significant difference between them, while T30 menisci had a significant decrease compared to T0 ($p < 0.05$, Fig. 7C). The adult showed markedly lower cellularity compared to T0 ($p < 0.001$, Fig. 7C) and to T10 ($p < 0.001$, Fig. 7C). Considering the meniscal areas, a decreasing trend of DNA content from T0 to adult animals was observed in AH, CB, and PH ($p < 0.001$, Fig. 7D).

No differences in cell efficiency were observed at T10 and T30 compared to T0, but cells in adult were significantly better performers than those in the other time point ($p < 0.001$ in adult vs T0/T10/T30, Fig. 7E). However, even if T30 showed some common characteristics with the adult one, the GAGs/DNA ratios underlined how the latter time point was the only one that showed a mature functional tissue in all considered meniscal areas ($p < 0.001$ in adult

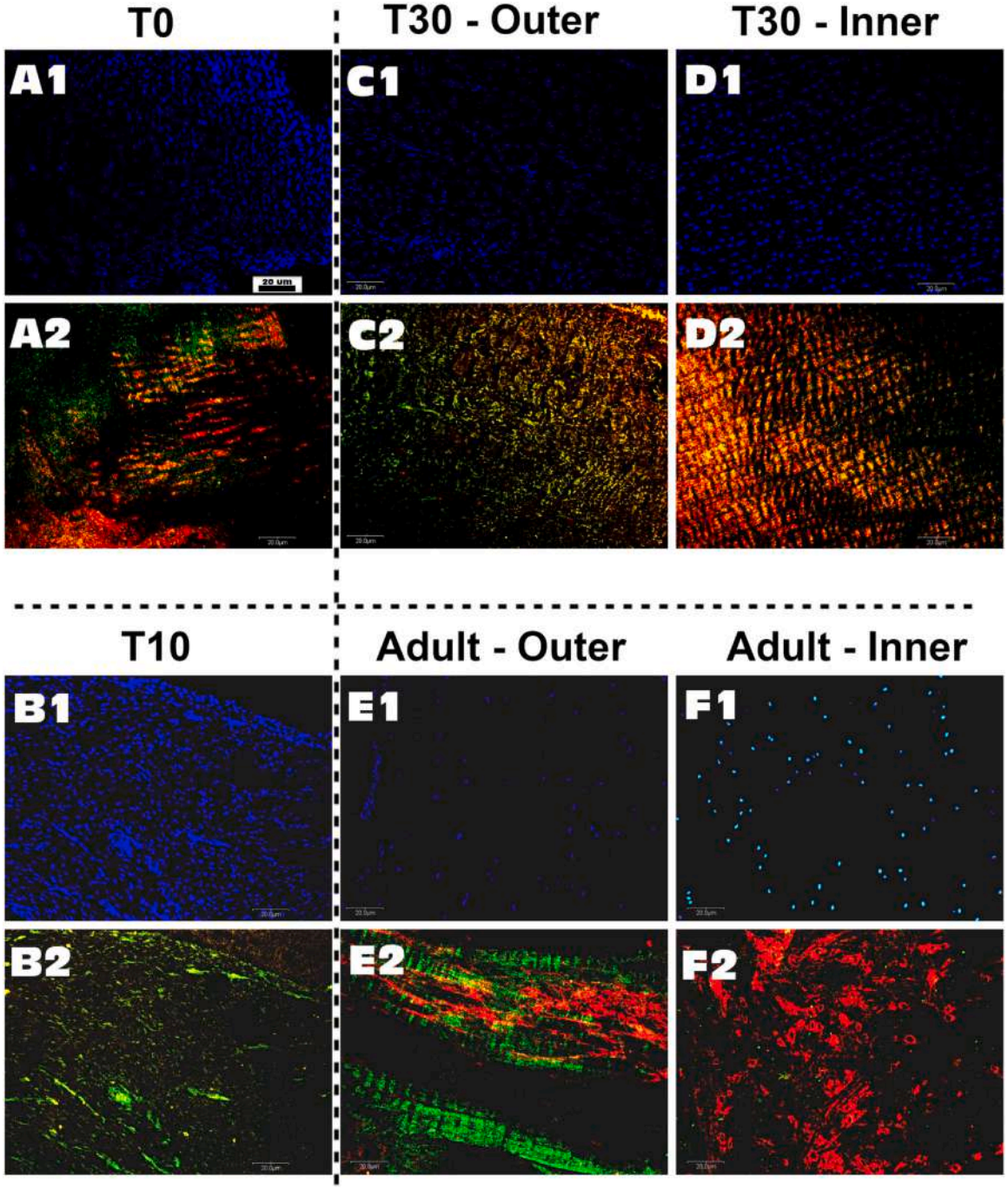

Fig. 5. Double-immunofluorescence of collagen type I and collagen type II. A1) T0 – medial meniscus, posterior horn, DAPI. A2) T0 – medial meniscus, posterior horn, collagen type I and type II. B1) T10 – medial meniscus, posterior horn, DAPI. B2) T10 – medial meniscus, posterior horn, collagen type I and type II. C1) T30 – medial meniscus, posterior horn, outer zone, DAPI. C2) T30 – medial meniscus, posterior horn, outer zone, collagen type I and type II. D1) T30 – medial meniscus, posterior horn, inner zone, DAPI. D2) T30 – medial meniscus, posterior horn, inner zone, collagen type I and type II. E1) Adult – medial meniscus, posterior horn, outer zone, DAPI. E2) Adult – medial meniscus, posterior horn, outer zone, collagen type I and type II. F1) Adult – medial meniscus, posterior horn, inner zone, DAPI. E2) Adult – medial meniscus, posterior horn, inner zone, collagen type I and type II. DAPI = blue nuclear staining; Collagen type I = green staining; Collagen type II: red staining; Co-expression of collagen type I and II: yellow staining. Scale bar = 20 µm.

vs T0/T10/T30 in AH, CB and PH, Fig. 7F) in which a small number of cells was able to produce a matrix rich of GAGs.

4. Discussion

Results of the present work add new information on the changes that accompany meniscus maturation, suggesting a specific response of meniscal cells to the mechanical stimuli of movement, load, and growth. The connective tissue changes that characterize the meniscus development occur mainly in the T10 - T30 interval and are well explained by the evaluation of the microstructure of the meniscus. SEM analysis revealed an initial bulgy structure at T0, which is probably due to the aggregation of clumps of collagen fibers that completely stretch only at T30, starting from the inner zone. Based on our results, the complete achievement of the "smooth" shape of the meniscus between T10 and T30 can be ascribed to the behavior of puppies during the postnatal period. In the first week, they crawl by dragging themselves on their venters with their forelimbs (Greer, 2014); at the turn of the first and the second week, they start using the hindquarters purposefully for propulsion (Greer, 2014).

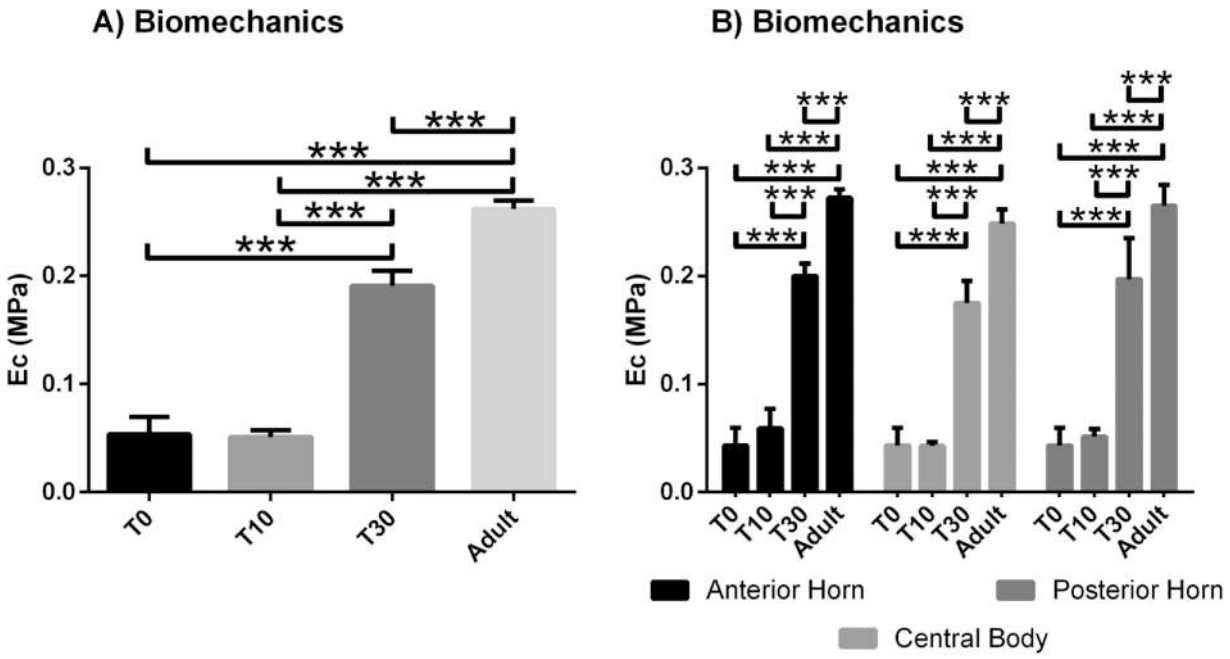

Fig. 6. Biomechanical evaluation of the meniscal samples using Young's Elastic Modulus in compression (Ec, MPa). A) Biomechanics at each experimental time. One-Way ANOVA was performed. B) Biomechanics considering the effect of anatomical was analyzed at the different studied time point; T0 is the same for the three portions; Two-Way ANOVA was performed. Values were expressed as mean ± S.E.M. * ** = $p < 0.01$.

The complete ability to walk on the four limbs is achieved between the third and fourth weeks of age (Greer, 2014). The described timing corresponds almost perfectly with our sampling points and the milestones achieved from the puppies are congruent with the structural modifications of the meniscus described in the current study. According to this, we can suggest that at birth, the meniscus appears bulbous because it is not subjected to any biomechanical forces. Actually, one of the main novelties of this study is the bulbous canine meniscus morphology that has not previously been observed in other species. The rapid change from clumped to stretched meniscal fibers in 30 days could represent a useful tool to study the effects of biomechanical forces acting on the tissue itself. Although the use of pet-derived material opens ethical issues, tissue cultures of waste material could help meniscal tissue engineering specifically and translational medicine in general. In human medicine, as early as 1983 Clark, Ogden (1983) observed several morphological changes of the meniscus starting from fetal samples up to adulthood, identifying biomechanics as one of the main influences on tissue differentiation. Also, our observations confirmed what Di Giancamillo et al. (2017) had described in pigs, namely that during growth the action of the different mechanical forces given by movement and exerted on the meniscus contribute to the differentiation of the tissue. The application of gait bearing may result crucial for the stretching of collagen fibers since the physiological intrauterine movements (characterized by non-weight bearing) described in dog fetuses (Kim and Son, 2007) do not seem to be enough.

Morphological analyses were used to study meniscal changes along the considered time points. Focusing on collagen fibers, Picro Sirius Red analysis revealed a change in collagen fibers' birefringence under polarized light during growth: T0, T10, and T30 menisci revealed bright and red-yellow fibers, which has been also observed collagen type I by immunofluorescence. This is in sharp contrast to what was observed in the adult group, which showed green fibers, weakly birefringent which are composed of type III collagen (Liu et al., 2021). Cury et al. (2016) reported a similar pattern of colors studying the changes in collagen types of adult and elderly rat tendons. The content of collagen III thus could vary markedly at different stages of development and disease. Wang et al. (2020) highlighted that collagen III is a necessary matrix constituent in mice meniscus; meniscal collagen III content decreases proportionately to the degree of degradation in humans (Mine et al., 2013). In this context, we suggest that green-matured fibers appear only in adult animals when meniscal development has been achieved.

Moreover, Safranin O Staining in T0 meniscus, reveals that the immature tissue shows associations of numerous elongated fibroblast-like cells and poor expression of matrix components. It achieves the physiological morpho-functional duality of mature tissue throughout cell phenotype changes and collagen regionalization: fibro-chondrocyte-like cells and prevalence of collagen type II, in the inner region vs fibroblast-like cells and co-expression of collagen type I and II in the outer one, as shown by double immunofluorescence.

We could observe that cells at T30 began to produce safranin O-positive matrix while biochemical analysis revealed that GAGs production decreased from T0 until the adult.

These results are an apparent discrepancy between the histochemical and biochemical data. What happens is that the histochemical staining reveals a matrix which, with age, becomes progressively positive for staining with Safranin O, i.e., the production of proteoglycans increases, while the biochemical data show a progressive reduction of glycosaminoglycans. To explain this phenomenon, it is necessary to consider that with the maturation of the tissue, the number of cells physiologically decreases, therefore a reduction of GAGs is also physiological. This is why we have chosen to consider the relationship between GAGs / DNA content as an index of cellular efficiency. Though the number of cells is indeed reduced (together with the effective content of GAGs), the remaining cells result functionally active, so much so that the efficiency ratio increases with age. The newborn has a significantly lower efficiency than the adult. This tissue maturation is compatible with what occurs in the hyaline cartilage (Mameri et al., 2022).

To complete the study on meniscal development, we decided to analyze the response to compressive forces during development as they reflect the maturation of the cellular component of the tissue, which becomes synthetically active creating a mature and functional matrix. Thanks to biomechanical analyses, we observed that in T0 -

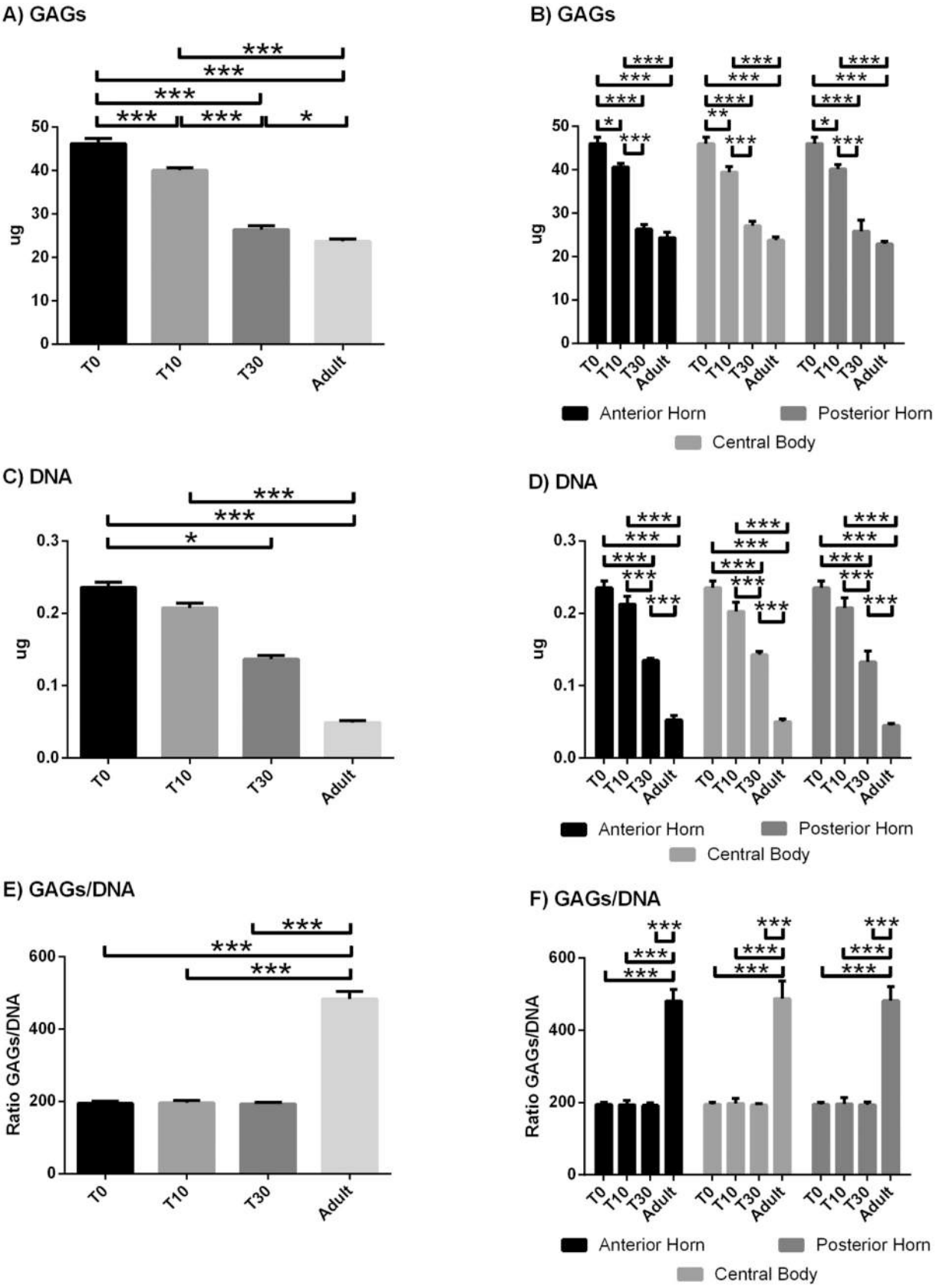

Fig. 7. Biochemical analysis. In A, C, and E the values within each experimental time were considered and One-Way ANOVA was performed. In B, D, and F the effect of the portion was analyzed at the different studied time point; T0 is the same for the three portions; in this case, Two-Way ANOVA was performed. Values were expressed as mean ± S.E.M. * = $p < 0.05$; ** = $p < 0,01$; *** = $p < 0.001$.

T30 groups, the elastic modulus was similar and low, since menisci are easily deformable and, consequently, they are not mature enough to resist the deformation caused by compression (Aidos et al., 2022). Finally, the adult meniscus revealed great resistance to compression: this ability is due to the fibro-chondrocytes maturation and subsequent deposition of the substances distributed in the extracellular matrix (Ferroni et al., 2021). In this case, the samples are hardly deformable, and the elastic modulus is high, indicating that the tissue can resist compression stimuli. These results are comparable to what has been previously seen in pigs (Aidos et al., 2022; Ferroni et al., 2021), thus indicating that the meniscus acquires the ability to counteract forces when all the components (cells and ECM) are already mature. Recently, Livet et al. (2022) evaluated the mechanical properties of the canine medial meniscus to understand their role within the stifle joint, improving early diagnosis of meniscal lesions. They found regional and radial variations for both the stiffness and the viscoelastic properties: the results indicated that the AH was significantly stiffer and less viscous than the CB and PH, but within the CB, the inner part was significantly stiffer than the periphery.

Our results indicate that knowing the morpho-functional mechanisms that determine the differentiation of a complex tissue such as the meniscal one is essential for the clinical application of new regenerative techniques. To date, meniscectomy still represents the gold standard in treatments of meniscal lesions due to the reduced regenerative capacity of the tissue, especially in the inner zone (Krupkova et al., 2018). In the field of regenerative and translational medicine, it is important to consider that patients with meniscal tears undergo pain and degenerative pathologies affecting the entire joint, such as rupture of the cruciate ligament (Barrett et al., 2005; Canapp, 2007) or osteoarthritis (Krupkova et al., 2018; Muir et al., 2007; Schwartz et al., 2011), in addition to the natural aging process (Francuski et al., 2014; Loeser, 2009). For this reason, over the past few years, there has been a growing tendency to preserve the meniscus whenever possible.

The limit of this work could have been the restricted number of dogs (experimental units), but the homogeneity of the breed was respected, and animals were used in compliance with the 3Rs principles. Moreover, it is still necessary to investigate meniscal development in dogs without lower limbs movement and weight-bearing.

5. Conclusions

This work demonstrates that during postnatal development the canine meniscus changes its structure and morphology. This is already detectable at 30 days of life: indeed, it is possible to observe how connective tissues quickly respond to mechanical stress. The peculiar bulbous shape of the newborn meniscus was not described in other animals at the same age, highlighting a species-specific feature of dog meniscus and should be deeply studied. The rapid phenotypic change of canine tissue could make it a good model to study the mechanisms leading to the differentiation of mature tissue. The chronological congruence of meniscal structure and puppies' postnatal behaviors may suggest the role of the biomechanical forces in the development of its ultimate shape and functions. Furthermore, this study is useful to fully understand the developmental biology of the meniscus for future reparative or regenerative applications in the field of veterinary medicine. This information results even more interesting since it can be helpful to study a translational model for humans.

Funding

This research did not receive any specific grant from funding agencies in the public, commercial, or not-for-profit sectors.

Ethical Statement

The cadavers used in the present study followed the guidelines of the E.U directive 2010/63/EU.

CRediT authorship contribution statement

Conceptualization: A.D.G., S.C.M.; methodology: clinical data collection and records, M.C.V.; macroscopic evaluation, histology, histochemistry, and double immunofluorescence: A.D.G., S.C.M., L.A., V.H, M.P.; SEM analysis: F.A.; biomechanics: U.P., F.B.; biochemical analyses: L.M., L.A., V.H.; validation, G.M.P. and S.C.M.; investigation: U.P., L.A., V.H., M.P.; data curation: A.D.G., writing – original draft preparation: A.D.G., S.C.M.; writing – review & editing, all; supervision: A.D.G., S.C.M., G.M.P.; project administration: A.D.G. All authors have read and agreed to the published version of the manuscript.

Declaration of Competing Interest

The authors declare that they have no known competing financial interests or personal relationships that could have appeared to influence the work reported in this paper.

References

Aidos, L., Modina, S.C., Millar, V.R.H., Peretti, G.M., Mangiavini, L., Ferroni, M., Boschetti, F., Di Giancamillo, A., 2022. Meniscus matrix structural and biomechanical evaluation: age-dependent properties in a swine model. Bioeng. Basel Switz. 9, 117. https://doi.org/10.3390/bioengineering9030117

Barrett, J.G., Hao, Z., Graf, B.K., Kaplan, L.D., Heiner, J.P., Muir, P., 2005. Inflammatory changes in ruptured canine cranial and human anterior cruciate ligaments. Am. J. Vet. Res. 66, 2073–2080. https://doi.org/10.2460/ajvr.2005.66.2073

Canapp, S.O., 2007. The canine stifle. Clin. Tech. Small Anim. Pract. 22, 195–205. https://doi.org/10.1053/j.ctsap.2007.09.008

Case, J.B., Hulse, D., Kerwin, S.C., Peycke, L.E., 2008. Meniscal injury following initial cranial cruciate ligament stabilization surgery in 26 dogs (29 stifles). Vet. Comp. Orthop. Traumatol. 21, 365–366. https://doi.org/10.3415/VCOT-07-07-0070

Clark, C.R., Ogden, J.A., 1983. Development of the menisci of the human knee joint. Morphological changes and their potential role in childhood meniscal injury. J. Bone Jt. Surg. - Ser. A 65, 538–547. https://doi.org/10.2106/00004623-198365040-00018.

Cury, D.P., Dias, F.J., Miglino, M.A., Watanabe, I., 2016. Structural and ultrastructural characteristics of bone-tendon junction of the calcaneal tendon of adult and elderly wistar rats. PLOS ONE 11, e0153568. . https://doi.org/10.1371/journal.pone.0153568

Danso, E.K., Oinas, J.M.T., Saarakkala, S., Mikkonen, S., Töyräs, J., Korhonen, R.K., 2017. Structure-function relationships of human meniscus. J. Mech. Behav. Biomed. Mater. 67, 51–60. https://doi.org/10.1016/j.jmbbm.2016.12.002

Deponti, D., Giancamillo, A. Di, Scotti, C., Peretti, G.M., Martin, I., 2015. Animal models for meniscus repair and regeneration. J. Tissue Eng. Regen. Med. 9, 512–527. https://doi.org/10.1002/term.1760.

Di Giancamillo, A., Deponti, D., Addis, A., Domeneghini, C., Peretti, G.M., 2014. Meniscus maturation in the swine model: changes occurring along with anterior to posterior and medial to lateral aspect during growth. J. Cell. Mol. Med. 18, 1964–1974. https://doi.org/10.1111/jcmm.12367

Di Giancamillo, A., Deponti, D., Modina, S., Tessaro, I., Domeneghini, C., Peretti, G.M., 2017. Age-related modulation of angiogenesis-regulating factors in the swine meniscus. J. Cell. Mol. Med. 21, 3066–3075. https://doi.org/10.1111/jcmm.13218

Ding, Z., Huang, H., 2015. Mesenchymal stem cells in rabbit meniscus and bone marrow exhibit a similar feature but a heterogeneous multi-differentiation potential: superiority of meniscus as a cell source for meniscus repair. BMC Musculoskelet. Disord. 16, 65. https://doi.org/10.1186/s12891-015-0511-8

Ferroni, M., Belgio, B., Peretti, G.M., Di Giancamillo, A., Boschetti, F., 2021. Evolution of meniscal biomechanical properties with growth: an experimental and numerical study. Bioeng. Basel Switz. 8, 70. https://doi.org/10.3390/bioengineering8050070

Fox, A.J.S., Bedi, A., Rodeo, S.A., 2012. The basic science of human knee menisci. Sports Health 4, 340–351. https://doi.org/10.1177/1941738111429419

Francuski, J.V., Radovanović, A., Andrić, N., Krstić, V., Bogdanović, D., Hadžić, V., Todorović, V., Macanović, M.L., Petit, S.S., Beck-Cormier, S., Guicheux, J., Gauthier, O., Filipović, M.K., 2014. Age-related changes in the articular cartilage of the stifle joint in non-working and working german shepherd dogs. J. Comp. Pathol. 151, 363–374. https://doi.org/10.1016/j.jcpa.2014.09.002

Frost-Christensen, L.N., Mastbergen, S.C., Vianen, M.E., Hartog, A., DeGroot, J., Voorhout, G., Wees, A.M.C., van, Lafeber, F.P.J.G., Hazewinkel, H. a W., 2008. Degeneration, inflammation, regeneration, and pain/disability in dogs following destabilization or articular cartilage grooving of the stifle joint. Osteoarthr. Cartil. 16, 1327–1335. https://doi.org/10.1016/j.joca.2008.03.013

Fukazawa, I., Hatta, T., Uchio, Y., Otani, H., 2009. Development of the meniscus of the knee joint in human fetuses. Congenit. Anom. 49, 27–32. https://doi.org/10.1111/j.1741-4520.2008.00216.x

Gamer, L.W., Xiang, L., Rosen, V., 2017. Formation and maturation of the murine meniscus. 1683–1689. J. Orthop. Res 35. https://doi.org/10.1002/jor.23446

Greer, M., 2014. Canine reproduction and neonatology. 1st Editionv, New York, Teton NewMedia. https://doi.org/10.1201/b17885.

Herrera Millar, V.R., Mangiavini, L., Polito, U., Canciani, B., Nguyen, V.T., Cirillo, F., Anastasia, L., Peretti, G.M., Modina, S.C., Di Giancamillo, A., 2021. Hypoxia as a stimulus for the maturation of meniscal cells: highway to novel tissue engineering strategies? Int. J. Mol. Sci. 22, 6905. https://doi.org/10.3390/ijms22136905

Hyde, G., Boot-Handford, R.P., Wallis, G.A., 2008. Col2a1 lineage tracing reveals that the meniscus of the knee joint has a complex cellular origin. J. Anat. https://doi.org/10.1111/j.1469-7580.2008.00966.x

Kim, B.-S., Son, C.-H., 2007. Time of initial detection of fetal and extra-fetal structures by ultrasonographic examination in Miniature Schnauzer bitches. J. Vet. Sci. 8, 289. https://doi.org/10.4142/jvs.2007.8.3.289

Koyuncu, E., Özgüner, G., Öztürk, K., Bilkay, C., Dursun, A., Sulak, O., 2017. The morphological anatomy of the menisci of the knee joint in human fetuses. Balk. Med. J. 34, 559–566. https://doi.org/10.4274/balkanmedj.2016.0081

Krupkova, O., Smolders, L., Wuertz-Kozak, K., Cook, J., Pozzi, A., 2018. The Pathobiology of the meniscus: a comparison between the human and dog. Front. Vet. Sci. 5. https://doi.org/10.3389/fvets.2018.00073

Liu, J., Xu, M., Wu, J., Zhang, H., Yang, L., Lun, D., Hu, Y., Liu, B., 2021. Picrosirius-polarization method for collagen fiber detection in tendons: a mini-review. Orthop. Surg. 13, 701–707. https://doi.org/10.1111/os.12627

Livet, V., Rieger, R., Viguier, É., Cachon, T., Boulocher, C., 2022. Micromechanical properties of the healthy canine medial meniscus. Res. Vet. Sci. 147, 20–27. https://doi.org/10.1016/j.rvsc.2022.03.018

Loeser, R.F., 2009. Aging and osteoarthritis: the role of chondrocyte senescence and aging changes in the cartilage matrix. Osteoarthr. Cartil. 17, 971–979. https://doi.org/10.1016/j.joca.2009.03.002

Makris, E.A., Hadidi, P., Athanasiou, K.A., 2011. The knee meniscus: structure––function, pathophysiology, current repair techniques, and prospects for regeneration. Biomaterials 32, 7411–7431. https://doi.org/10.1016/j.biomaterials.2011.06.037

Mameri, E.S., Dasari, S.P., Fortier, L.M., Verdejo, F.G., Gursoy, S., Yanke, A.B., Chahla, J., 2022. Review of meniscus anatomy and biomechanics. Curr. Rev. Musculoskelet. Med. 15, 323–335. https://doi.org/10.1007/s12178-022-09768-1

McNulty, A.L., Guilak, F., 2015. Mechanobiology of the Meniscus. J. Biomech. 48, 1469–1478. https://doi.org/10.1016/j.jbiomech.2015.02.008

Melrose, J., Smith, S., Cake, M., Read, R., Whitelock, J., 2005. Comparative spatial and temporal localisation of perlecan, aggrecan and type I, II and IV collagen in the ovine meniscus: an ageing study. Histochem. Cell Biol. 124, 225–235. https://doi.org/10.1007/s00418-005-0005-0

Mikic, B., Johnson, T.L., Chhabra, A.B., Schalet, B.J., Wong, M., Hunziker, E.B., 2000. Differential effects of embryonic immobilization on the development of fibrocartilaginous skeletal elements. J. Rehabil. Res. Dev. 37, 127–133.

Mine, T., Ihara, K., Kawamura, H., Date, R., Umehara, K., 2013. Collagen expression in various degenerative meniscal changes: an immunohistological study. J. Orthop. Surg. 21, 216–220. https://doi.org/10.1177/230949901302100221

Muir, P., Oldenhoff, W.E., Hudson, A.P., Manley, P.A., Schaefer, S.L., Markel, M.D., Hao, Z., 2007. Detection of DNA from a range of bacterial species in the knee joints of dogs with inflammatory knee arthritis and associated degenerative anterior cruciate ligament rupture. Microb. Pathog. 42, 47–55. https://doi.org/10.1016/j.micpath.2006.10.002

Peretti, G.M., Polito, U., Di Giancamillo, M., Andreis, M.E., Boschetti, F., Di Giancamillo, A., 2019. Swine meniscus: are femoral-tibial surfaces properly tuned to bear the forces exerted on the tissue. Tissue Eng. Part A 25, 978–989. https://doi.org/10.1089/ten.tea.2018.0197

Polito, U., Peretti, G.M., Di Giancamillo, M., Boschetti, F., Carnevale, L., Veronesi, M.C., Sconfienza, L.M., Agnoletto, M., Mangiavini, L., Modina, S.C., Di Giancamillo, A., 2020. Meniscus matrix remodeling in response to compressive forces in dogs. Cells 9, 265. https://doi.org/10.3390/cells9020265

Proctor, C.S., Schmidt, M.B., Whipple, R.R., Kelly, M.A., Mow, V.C., 1989. Material properties of the normal medial bovine meniscus. J. Orthop. Res. 7, 771–782. https://doi.org/10.1002/jor.1100070602

Proffen, B.L., McElfresh, M., Fleming, B.C., Murray, M.M., 2012. A comparative anatomical study of the human knee and six animal species. Knee 19, 493–499. https://doi.org/10.1016/j.knee.2011.07.005

Ribitsch, I., Peham, C., Ade, N., Dürr, J., Handschuh, S., Schramel, J.P., Vogl, C., Walles, H., Egerbacher, M., Jenner, F., 2018. Structure—Function relationships of equine menisci. PLOS ONE 13, e0194052. . https://doi.org/10.1371/journal.pone.0194052

Schwartz, Z., Zitzer, N.C., Racette, M.A., Manley, P.A., Schaefer, S.L., Markel, M.D., Hao, Z., Holzman, G., Muir, P., 2011. Are bacterial load and synovitis related in dogs with inflammatory stifle arthritis. Vet. Microbiol. 148, 308–316. https://doi.org/10.1016/j.vetmic.2010.09.011

Sosio, C., Di Giancamillo, A., Deponti, D., Gervaso, F., Scalera, F., Melato, M., Campagnol, M., Boschetti, F., Nonis, A., Domeneghini, C., Sannino, A., Peretti, G.M., 2015. Osteochondral repair by a novel interconnecting collagen–hydroxyapatite substitute: a large-animal study. Tissue Eng. Part A 21, 704–715. https://doi.org/10.1089/ten.tea.2014.0129

Tsinman, T.K., Jiang, X., Han, L., Koyama, E., Mauck, R.L., Dyment, N.A., 2021. Intrinsic and growth-mediated cell and matrix specialization during murine meniscus tissue assembly. FASEB J. . Publ. Fed. Am. Soc. Exp. Biol. 35, e21779. . https://doi.org/10.1096/fj.202100499R

Uhthoff, H.K., Kumagai, J., 1992. Embryology of Human Meniscus, in: Trends in Research and Treatment of Joint Diseases. Springer, Japan, Tokyo, pp. 135–141. https://doi.org/10.1007/978-4-431-68192-2_17

Wang, C., Brisson, B.K., Terajima, M., Li, Q., Hoxha, K., Han, B., Goldberg, A.M., Sherry Liu, X., Marcolongo, M.S., Enomoto-Iwamoto, M., Yamauchi, M., Volk, S.W., Han, L., 2020. Type III collagen is a key regulator of the collagen fibrillar structure and biomechanics of articular cartilage and meniscus. Matrix Biol. Matrix Biomech. 85–86, 47–67. https://doi.org/10.1016/j.matbio.2019.10.001

Yu, H., Adesida, A.B., Jomha, N.M., 2015. Meniscus repair using mesenchymal stem cells - a comprehensive review. Stem Cell Res. Ther. 6, 86. https://doi.org/10.1186/s13287-015-0077-2